International Journal of Innovative
Computing, Information and Control
Volume **13**, Number **4**, August **2017**

 ISSN 1349-4198
pp. **1289–1306**

A NOVEL WIRELESS ACOUSTIC EMISSION SENSOR SYSTEM FOR DISTRIBUTED WOODEN STRUCTURAL HEALTH MONITORING

Yin Wu[1], Wenbo Liu[2] and Kaiyu Li[2]

[1]College of Information Science and Technology
Nanjing Forestry University
No. 159, Longpan Road, Nanjing 210037, P. R. China
wuyin@njfu.edu.cn

[2]College of Automation
Nanjing University of Aeronautics and Astronautics
No. 29, Jiangjun Avenue, Nanjing 211106, P. R. China
{ wenboliu; LKY_401 }@nuaa.edu.cn

Received December 2016; revised April 2017

Abstract. *This paper presents the development of a novel wireless acoustic emission (AE) sensor platform designed for distributed large-scale wooden structure health monitoring. A set of AE sensors is deployed at the surface of the wooden components, and the proposed wireless AE network is continuously monitoring and inspecting the AE propagation characteristics within the structure to identify damages. The proposed platform features an ARM processor of STM32F407 with real-time data sampling rate up to 5Msps and an improved IEEE 802.11 b/g/n wireless data transceiver CC3200 with up to 6Mbps data rate. Besides, embedded signal sampling and data processing algorithms to extract AE signal features are also introduced, especially a simplified difference encoding data compression algorithm is used to reduce the data transmission amount whilst maintains the high sensitivity and reliability. Then damage identification running in the base station analyzes the AE signals' distinctions in the pressure injury of wooden component. At last, the sensor performance, in terms of data sampling and fault detection, has been analyzed by means of experimental results.*

Keywords: Acoustic emission, Wireless sensor network, Wooden structure, Structural health monitoring, Signal processing, Data compression

1. **Introduction.** Wood has been used as a structural material since ancient times. Timber building members are an integral part of almost all historic buildings, serving particularly as columns, beams and roof structures in China [1]. Their condition has a great influence on the working life of the entire building; therefore, it is important to continually monitor it and timely capture any negative changes. Given the historical value of many wooden buildings, the methods required for the investigation of their current condition should not unnecessarily interfere with the existing structures. So far, visual assessment has primarily been used. However, to determine the internal condition of a structure, or to quantify its physical and mechanical properties, more precise methods are needed. Among them, the most commonly used technique is acoustic emissions [2-4].

Acoustic emissions (AE) are the stress waves produced by the sudden internal stress redistribution of the materials caused by the changes in the internal structure. Possible causes are crack initiation and growth, crack opening and closure, dislocation movement, twinning, and phase transformation in monolithic materials and fiber breakage and fiber-matrix deboning in composites [5]. Monitoring systems listen to AE signal and perform

frequency/time domain signal processing to identify fault pattern in the early stage of surface/subsurface crack formation. Most of the sources of AE are damage-related; thus, the detection and monitoring of these emissions are commonly used to predict material failure. This technique has been widely applied in materials testing, structure health monitoring (SHM): such as bridges, towers, and pavilions [6-9]. However, as the transmission of AE signals needs cables for common commercial AE instruments, it is very inconvenient for the AE testing and monitoring of large scale structures. So in order to satisfy the requirement of AE testing and monitoring for timber construction, we have developed an advanced multichannel wireless AE system with large transmitting rate and synchronous clock based on the Wi-Fi and real time clock (RTC) mechanisms. This paper reports the details of the developed wireless AE system.

Recently, some researches have focused on the wireless AE technique for damage identification or impact localization for SHM. A. Ledeczi et al. [10] presented a prototype wireless AE system for the detection of active fatigue cracks in aging railways bridges, the node has 4 channels with maximum sampling rate 3MHz, but the transmitting rate was only 250 kbps. O. M. Bouzid et al. [11,12] developed a wireless AE system for wind turbine blades, it was comprised of MICAz motes equipped with the sensor board (MTS310), and it ran a content-based AE signal features extraction algorithm, which leads to a low sampling rate much lower than the Nyquist rate. Results showed that it could locate AE events precisely with its localization model. M. D. Prieto et al. [13] introduced a novel self powered wireless sensor applied to condition monitoring of gears by means of AE analysis, and 3 AE channels were connected to a 14-bit analog to digital (AD) converter. A fixed sampling frequency of 2MHz during time windows of 10ms was applied, resulting in 280Kbits of data, and a spectral resolution of 100Hz. On the other hand, as for the nondestructive testing of wooden structures, J. V. Oliver-Villanueva and M. A. Abian-Perez [14] designed a wireless sensor which could be installed in the wood component to collect the temperature, humidity and illuminance of its circumstance, and also it could be used to pre-warn the activity of termites and other insect pests. While Y. Fujii et al. have studied the AE signal feature of termite in the wood since 2007 [15-17], and their research indicates that AE method shows great performance in terms of collecting waves of termite activity. However, as far as we know, there has no wireless AE sensor designed for wooden structure monitoring to date, and the main challenges are: the damage modes of wooden component in the historic building can be composed of many types, such as matrix cracking, delamination, fiber breakage and debonding. Each has its own special acoustic property and apparently these different damages map with different corresponding AE signals. However, in reality, damages always show up in a combination form with overlapping characteristics of different types; in addition, due to the anisotropic propagation nature of wood and the ever-present multi-source noise pollution, all make the AE signal acquisition and identification in wooden component a highly difficult task.

As a result of the work discussed above, we can figure that conventional design of wireless sensor node is not suitable for nondestructive sensing in SHM, where the AE signal to be detected always has a high frequency (perhaps even reach several hundred KHZ). Therefore, these requirements are needed.

(i) High sampling rate and communication rate. When AE events occur, the sensor node should acquire the raw wave data as much as possible. After then, it should transmit the data to a center server that carries out centralized data processing and damage identification algorithms as soon as possible. However, due to the complexity of AE signal in wooden structure [18], the existing wireless sensor mote (such as MicaZ, TelosB) and wireless communication protocol (such as IEEE 802.15.4) cannot afford such high sampling rate and communication rate.

(ii) Efficient data flow management and data compression algorithm. When lots of AE wave data arrive, the node should decide whether transmitting it directly to the center server or holding on for next analysis if necessary. Besides in the view of economic operation: reducing the data traffic, saving the energy of the node and prolonging network lifetime, we should compress the data awaiting transmission as much as possible.

(iii) Precise time synchronization. When an AE wave is detected, the absolute arriving time is always different between sensors mounted in different area, so we could locate the AE source by using the time-of-flight (TOF) algorithm [19]. The accuracy of AE signal arrival time and the resolution of damage localization are greatly influenced by the errors in time synchronization.

So to address the challenges of these requirements, we have developed a new wireless AE sensor platform. It features an ARM based STM32F407 processor with up to 5Msps sampling rate and an IEEE 802.11 b/g/n based wireless data transmitter CC3200 with up to 6Mbps data rate. Each node supports up to 2 AE channels. Furthermore, embedded data acquisition and processing frame is presented, especially the simplified difference encoding data compression algorithm which reduces the wireless transmission payload by 50%. As well fracture feature analysis program running in the center server is also able to identify the status of damage and locate the AE source.

This paper is organized as follows. Next section will present a detailed description of the sensor node requirements and design. Then, an overview of the overall system architecture and operation is presented, and then followed by a summary of the experiment results and offline data evaluation methodology. At last the paper concludes with shortcomings and our planned future work.

2. **Sensor Node Architecture and Operation.**

2.1. **Sensor node hardware schematic.** The prototype design is illustrated in Figure 1. The wireless AE node mainly consists of two parts, namely, ARM base board, and radio board. In base board, one outstanding feature of the microcontroller STM32F407 is the capability of high speed data sampling. The direct memory access (DMA) unit on STM32F407 allows the wireless AE node to collect sensor data at 5Msps. On the other hand, the radio board contains microcontroller CC3200, RTC chip DS3232M.

(i) Base board. A wireless AE sensor node always runs embedded computation intensive programs, e.g., high speed sampling procedure. So the base board should be designed on the basis of these requirements: high frequency microcontroller, certain memory cache, DMA controller, SPI and IIC interface. For our platform, we choose the ARM Cortex M4 core chip because of its low cost and low power.

The base board is a four-layer PCB roughly with the size of 9.7cm by 6.6cm. It adopts an ST microcontroller STM32F407VGT6 (features a floating point unit) working at 168MHz. Thus, on-board high-sampling data acquisition and processing are entirely possible. In this board, the SPI1 interface is used to communicate with radio board, and PC2 analog interface is used for acquiring sensor data, respectively.

(ii) Radio board. A Texas Instrument microcontroller CC3200 is chosen. It is made up of an ARM Cortex M4 core and an ultra low power Wi-Fi network processor CC3100. This chip is operating at a maximum frequency of 80MH with a maximum data rate of 6Mbps.

The radio board uses SPI bus (P05, P06, P07, and P45) to receive sensor data from the base board. It is also a four-layer PCB and the size is 9.4cm×5.8cm roughly. In transmitting state, the radio board consumes 755mW of power (229mA of power at 3.3V) but less than 200mW of power (59mA of power at 3.3V) in receiving mode.

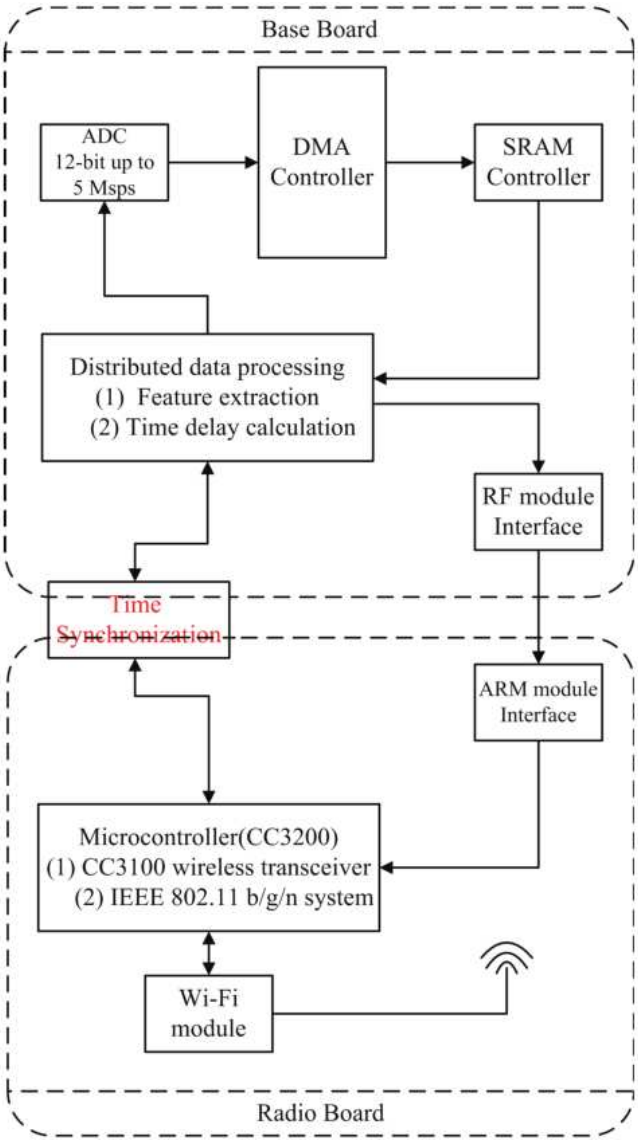

FIGURE 1. Block diagram of the sensor node

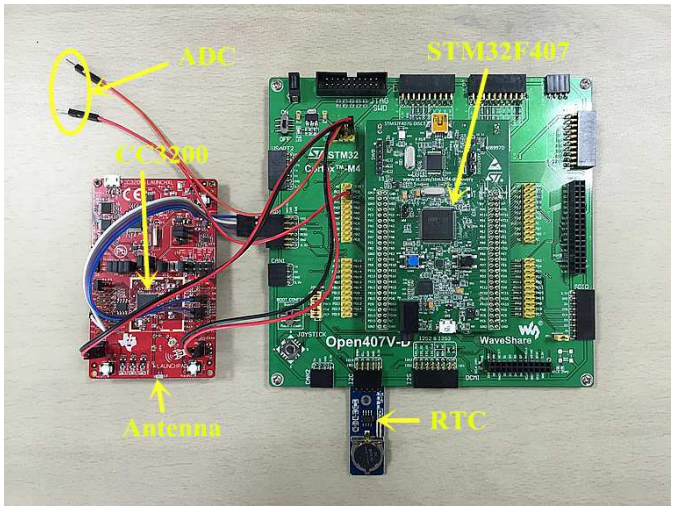

FIGURE 2. Prototype of the sensor node

Another task of the radio module is time synchronization. Here we use DS3232M as node's clock source; it is an extremely accurate RTC with ±5ppm. The CC3200 on radio board only takes wireless communication and time synchronization task, while the STM32F407 on base board takes the computation-intensive data processing task. Only this dual-core architecture can guarantee the effective and efficient working of both controllers because lots of interrupts exist; thus a precise time synchronization can be achieved. The prototype of our sensor node is shown in Figure 2.

2.2. **Sensor node software architecture.** The process diagram illustrates the main working stages of wireless AE node, as shown in Figure 3. It begins with the data

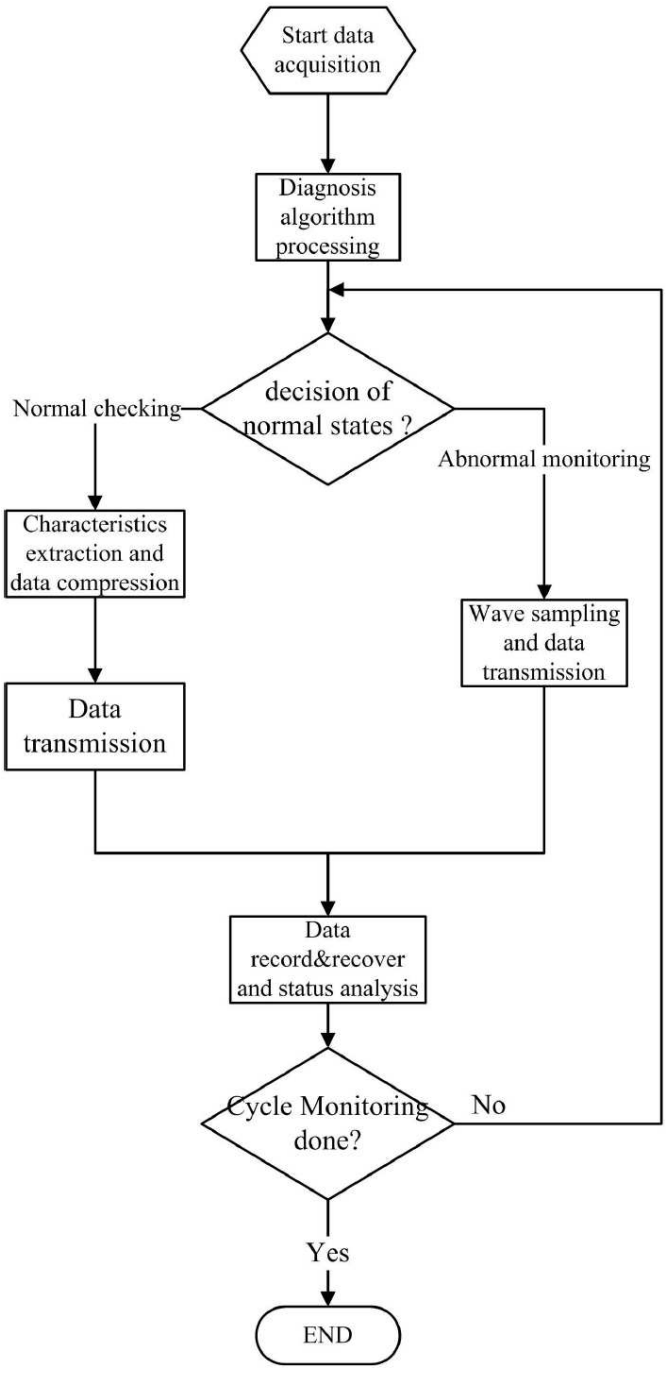

FIGURE 3. Operating cycle carried out by the node

acquisition of AE signal after receiving the "START" command from control center. At this stage, data about the sensing signal is collected from the AE sensor. Then, diagnosis algorithm is executed to compute the AE event features. If the activity and intensity show in a normal range, the node will enter "normal checking" workflow, it will extract the data characteristics and compress it to save transmission payload, and only after this, the wireless communication from node to the control center will begin; however, if in an abnormal state, the node will enter "closely monitoring" stage, the acquired raw data will be transferred directly to the control center as soon as possible, and there is no data compression procedure here. Then the following process is operated in control center. In here, the characteristics are recovered and recorded for next operation or the signal is calculated for advanced analysis. Finally, feature extraction and damage localization are carried out to compute the health status of whole structure.

The specification of our simplified difference encoding data compression algorithm is introduced as follows.

As for most normal checking stage, the AE signal amplitudes are small even close to zero. In fact, they remain steady most of the time until turning into the closely monitoring stage when emergencies happen. So it is unnecessary to transfer all the extracted values each time, while just need to transfer the difference between current value and the last value. With regard to our wireless AE sensor network, the extracted characteristic values are amplitude, rise time, duration, ring count, hit count and power (see part 4.1 for detail), and thus the format of data package should be as follows.

TABLE 1. The format of data package without compression

Package No	Amplitude	Rise time	Duration	Ring Count	Hit Count	Power	Checksum
1 byte	2 byte	2 byte	2 byte	2 byte	2 byte	2 byte	1 byte

However, after adopting difference encoding algorithm, the format is like this.

TABLE 2. The format of data package with compression

Package No	Flag byte	Amplitude	Rise time	Duration	Ring Count	Hit Count	Power	Checksum
1 byte	1 byte	1 byte	1 byte	1 byte	1 byte	1 byte	1 byte	1 byte

The flag byte represents whether to transmit amplitude, rise time, duration, ring count, hit count and power's data or not. If the difference between current value and the last value is zero, then we will not forward the data, and just set the corresponding bit in the flag to zero. For example, suppose the difference is amplitude: 5.0, rise time: 2.2, duration: 4.0, ring count: 0.0, hit count: 0.0 and power: 5.9, then the transmission package is shown as follows.

TABLE 3. The example format of data package with compression

Package No	Flag byte	Amplitude	Rise time	Duration	Power	Checksum
1 byte	000100111	1 byte	1 byte	1 byte	1 byte	1 byte

The above compressed package has only 7 byte; apparently the expected data compression effect is achieved. In this difference encoding algorithm, the minimum package number is 3 byte, the maximum number is 9 byte, that is to say, the max compression ratio is 78.6% and the min is 35.7%. And after all, it is a lossless style without any data

loss. For the recover port, it could easily recognize the data meaning in regards to the package length.

As soon as radio board gets the above acquired data from base board by SPI interface, it will fill these data into the payload format. Then all the network address, MAC address, and application payload are packaged inside the standard IEEE 802.11 data frame. Once the payload has been filled to the full, wireless packet will be sent to the control center.

3. **System Architecture and Management.** Different from the traditional SHM system which is based on Fiber Bragg Grating sensors, wireless AE sensor network for SHM has three advantages: (i) the energy used for detection comes from the structure itself; (ii) highly-sensitive to the structural deficiency; (iii) saving the trouble of signal wire arrangement.

The framework diagram of our wireless AE sensor network is illustrated in Figure 4(a). It mainly includes the following units: (i) AE sensors to transform the responding elastic AE waves into an electrical signal; (ii) wireless AE node. Each node is able to connect to two AE sensors; it always runs distributed data processing program for information extraction and analysis; also each node should keep time synchronization for improving the damage localization accuracy; then all nodes form a network and send data to the control center (base station); (iii) control center. It is in charge of establishing and maintaining the Wi-Fi network, collecting each node's transmission data, launching time synchronization mechanism, processing and analyzing damage identifications. Thus, the proposed wireless AE sensor network allows an autonomous and continuous onsite monitoring and diagnosis of wooden structures.

Figure 4(b) shows an installation diagram of wireless AE WSN in a wooden temple.

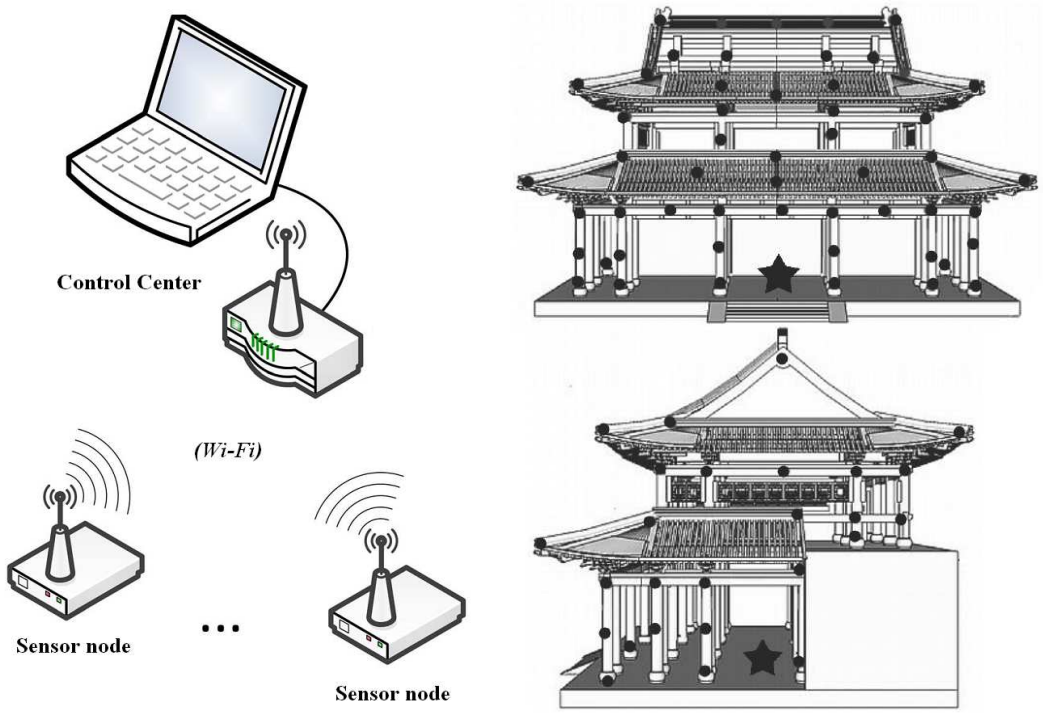

(a) (b)

FIGURE 4. (a) Framework diagram of the wireless AE sensor network; (b) installation diagram in wooden temple: black dot represents wireless AE node, pentagram represents control center (base station)

As soon as the wireless communication network has been established, time synchronization procedure should be carried out to ensure that all wireless AE nodes are well synchronized and a standard time has been achieved. Once the network is set up and all nodes are online, the control center first broadcasts the start time to all nodes. And the nodes should write the time data into their RTC chip simultaneously to keep alive. After sending start time, the control center waits for receiving data from all nodes. So upon receiving the start time from control center, nodes will switch from listening state to a pre-working state, when the RTC task is completed, nodes would send an "OK" message back to control center. After that, a "START" command will broadcast to all nodes. Then all the wireless AE nodes start data acquisition of AE signals.

4. **Proof-of-Concept Tests and Performance Evaluation.** For purpose of assessing the performance of the proposed wireless AE sensor node, several proof-of-concept lab tests have been implemented and the results are given subsequently. As continuous online monitoring obviously is required, the use of wireless sensing systems requires approaches for decentralized data processing (i.e., the on-board wireless units). In this case, firstly, we want to test that important AE features can be locally extracted from the raw data and only those features to be sent to the control center. Next, the transmission of raw AE waves is verified, including normal and high sampling rate. At last, we want to distinguish AE signal characteristics in different fracture stages.

The lab test platform is shown in Figure 5: it consists of a computer working as the control center and graphic user interface (namely this computer establishes and maintains the Wi-Fi network) and the designed wireless AE node. More often than not, a conditioning board needs to be installed between the AE sensor and ADC converter to attain impedance matching, but as our focus is to verify the distributed signal processing

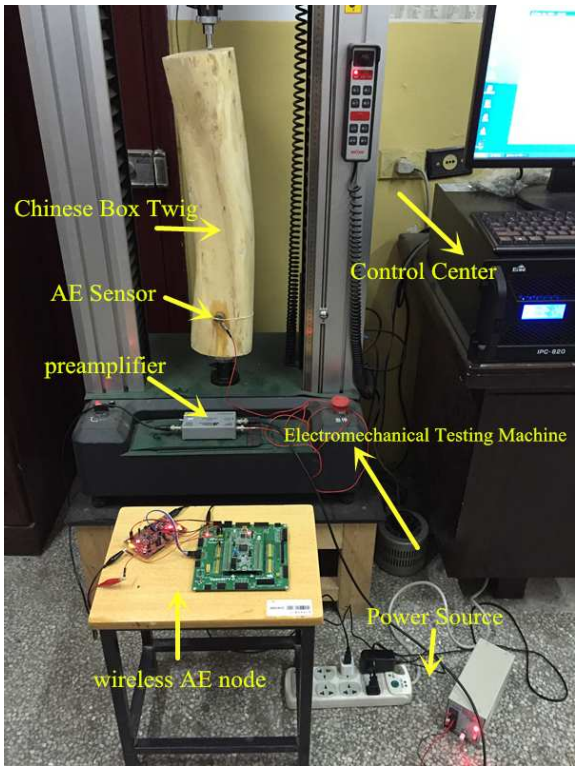

FIGURE 5. Lab test platform for the wireless AE sensor network

and wireless transmission, we replace it with a voltage preamplifier from "Physical Acoustics Inc. [20]" in this lab test. At last one AE sensor R15a is attached to the surface of a boxwood specimen (80cm high, 15cm diameter), and mounted on an electromechanical universal testing machine together. Once if a strike acts on the boxwood specimen, we should receive AE data on the control center immediately.

4.1. **AE feature extraction.** As it is known, AE waves are abnormal and transient activities, which are affected by the characteristics of the induced stress field. These waves can be converted into a number of useful AE parameters or features, as shown in Figure 6, which can then be used to identify these events. Some of these parameters are as follows [21].

(i) Amplitude, A, is the maximum amplitude which is usually measured in decibels (dB).

(ii) Rise time, R, is the time interval between the first threshold crossing and the time when the AE signal reaches its amplitude.

(iii) Duration, D, represents the time difference between the first and the last crossings of the threshold value.

(iv) Ring count, RN, refers to the number of times the signal crosses the threshold value.

(v) Hit count, HN, refers to the number obtained by counting each discerned AE event once.

(vi) Power, P, is the area under the curve or the summation of the squared sample values.

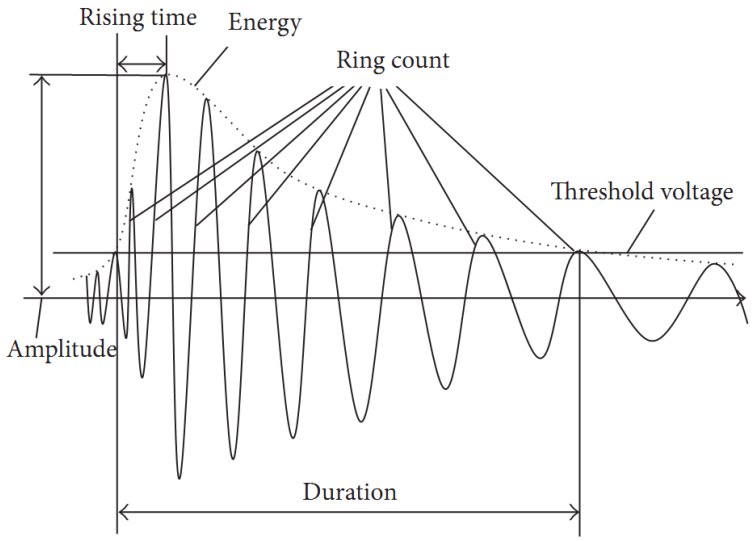

FIGURE 6. Definition of simplified waveform parameters of AE signal

Then we set the AE sensor with these parameters (sampling frequency 1M HZ, sampling number 1k, threshold voltage 30dB) and set the electromechanical universal testing machine with parameters (5mm/min, 10KN) to carry out a wood hardness testing, simultaneously the feature extraction results can be found out on the control center, and part of it is shown in Table 4.

Figure 7 provides the curves of loading and cumulative hit counts changing in time, we can see that the two present similar variation trend. And it shows that our node is highly sensitive to the response of boxwood specimen under press testing.

TABLE 4. Part of AE feature extraction results

NO	A (dB)	R (μs)	D (μs)	RN	P (mv*ms)	Time (year/month/dateclock /minute/secondnum)
31	30.2	49	113	2	0.3	20160721-135012-062
138	98.5	50	4687	9	5607.2	20160721-135015-599
227	32.5	11	33	5	0.1	20160721-135018-185
294	65.5	55	4668	12	3836.9	20160721-135019-605

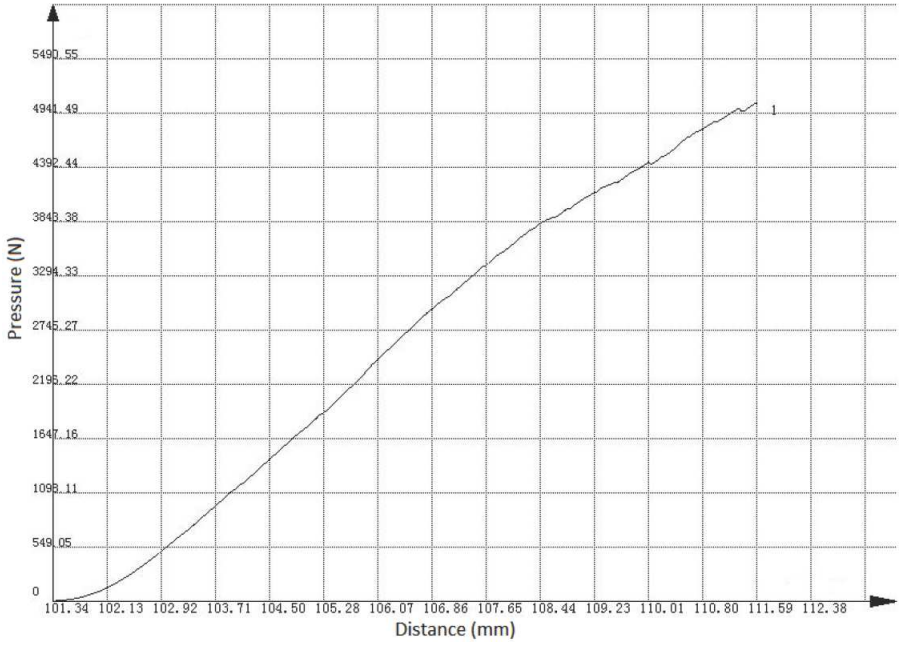

(a)

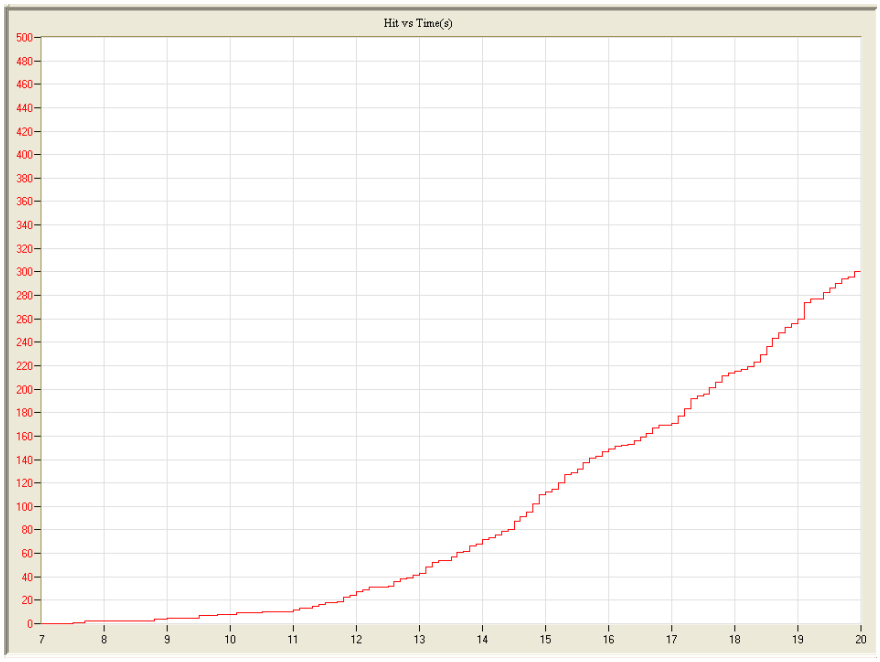

(b)

FIGURE 7. (a) Loading variation over distance, (b) the cumulative number of hit counts over time

4.2. **Wave sampling and transmission.** In this phase, we set the AE sensor with these parameters (sampling frequency 1M/5M HZ, sampling number 1k, threshold voltage 30dB), and make it transmit all the waves it has captured. Then we use a joiner hammer to knock at the front end of the boxwood specimen several times, and the AE waves received are shown in Figure 8.

Obviously, Figure 9 shows more specific details of waves than Figure 8, so we mainly use this sampling approach in closely monitoring state. However, it is also notable that the energy consumption is much higher than normal sampling approach.

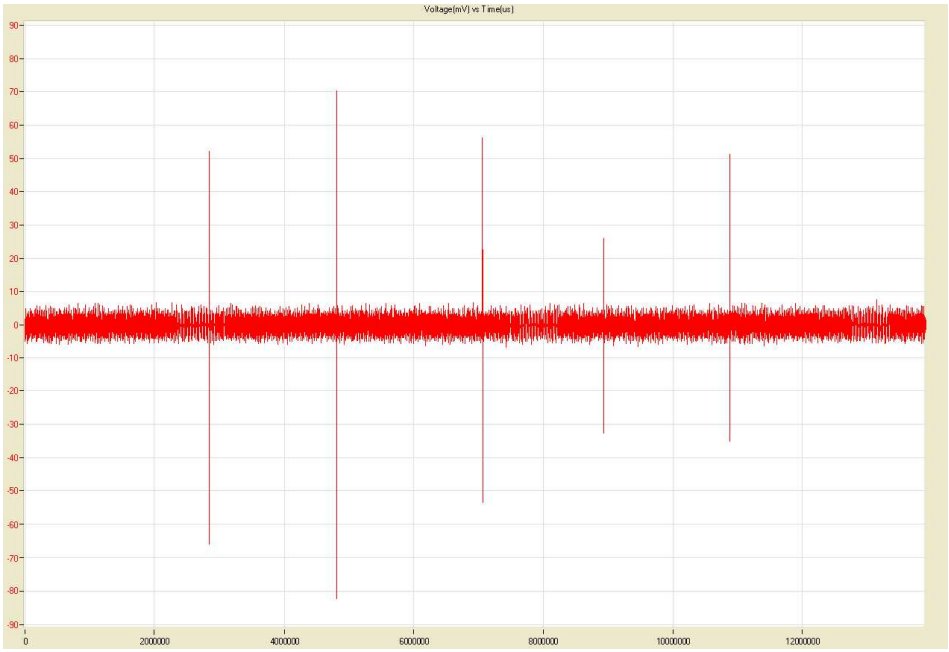

(a)

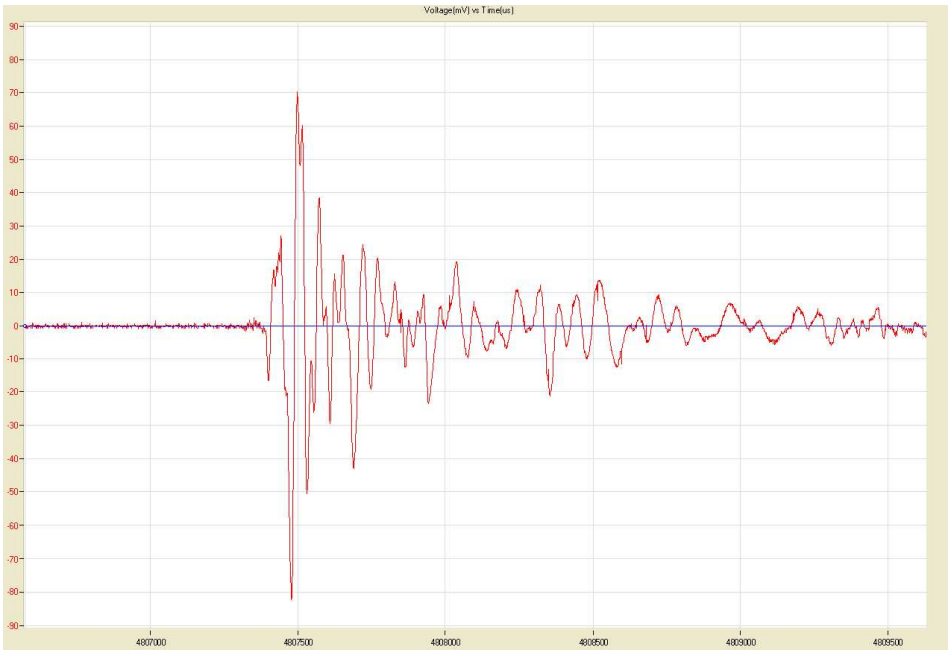

(b)

FIGURE 8. (a) All the 5 hits waves when sampling at 1MHZ, (b) the second hit wave

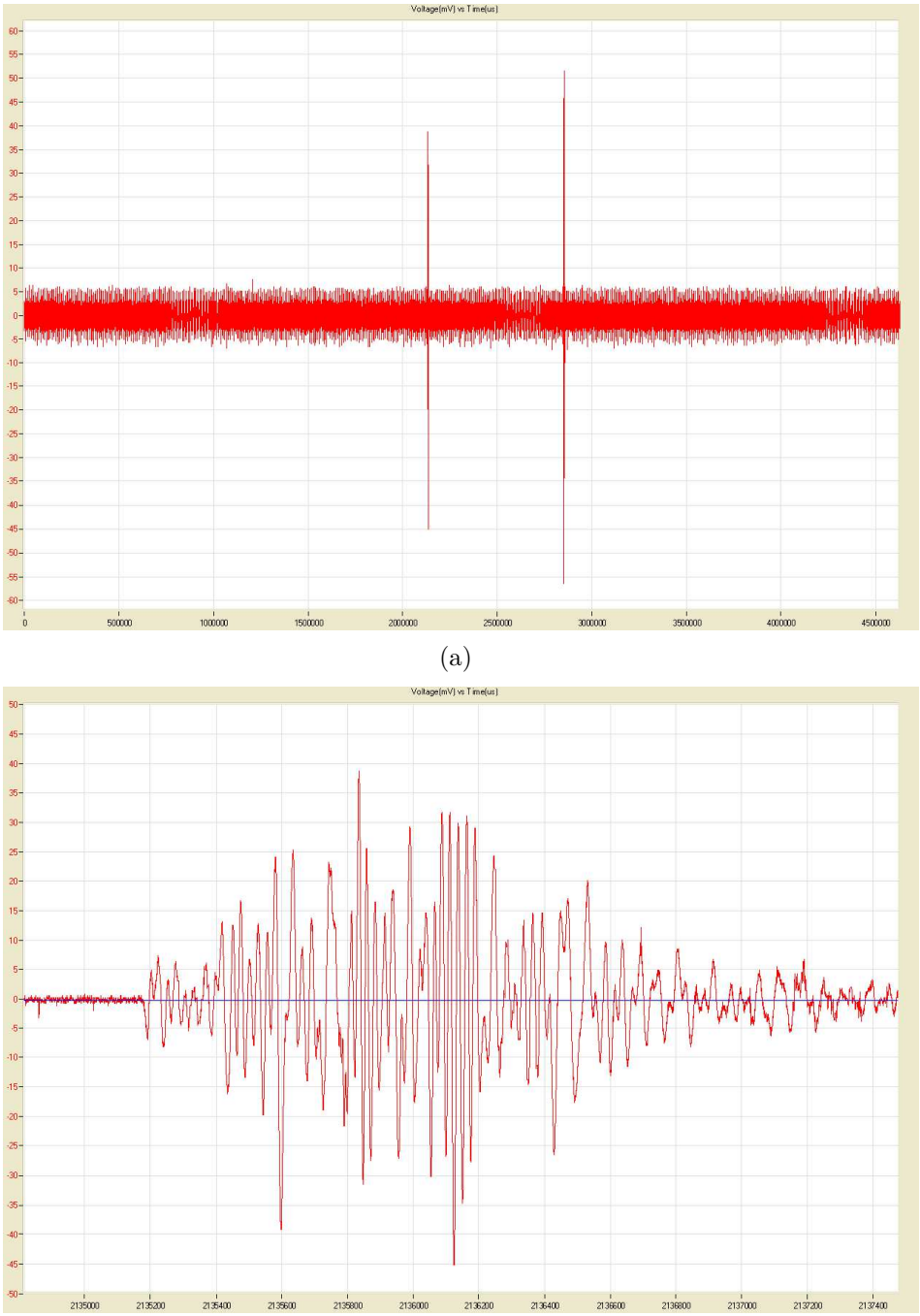

(a)

(b)

FIGURE 9. (a) All the 2 hits waves when sampling at 5MHZ, (b) the first hit wave

After these experiments, we connect two AE sensors on the wireless node; one is mounted near the front end, while the other near the bottom end, then we knock the boxwood specimen on the front end several times again, and the waves received are shown in Figure 10. And from Figure 11 it is evident that the two AW waves arrive at different time, so we can calculate TOF accurately.

At the end of this phase, we have a comparison of our wireless sensor with a standard product (PCI-2 AE system from Physical Acoustics Inc. [22]). For convenience of analysis, we place two sensors close to each other near the front end of specimen, and wired with the two different systems individually, then we carry out a hit on the specimen and the

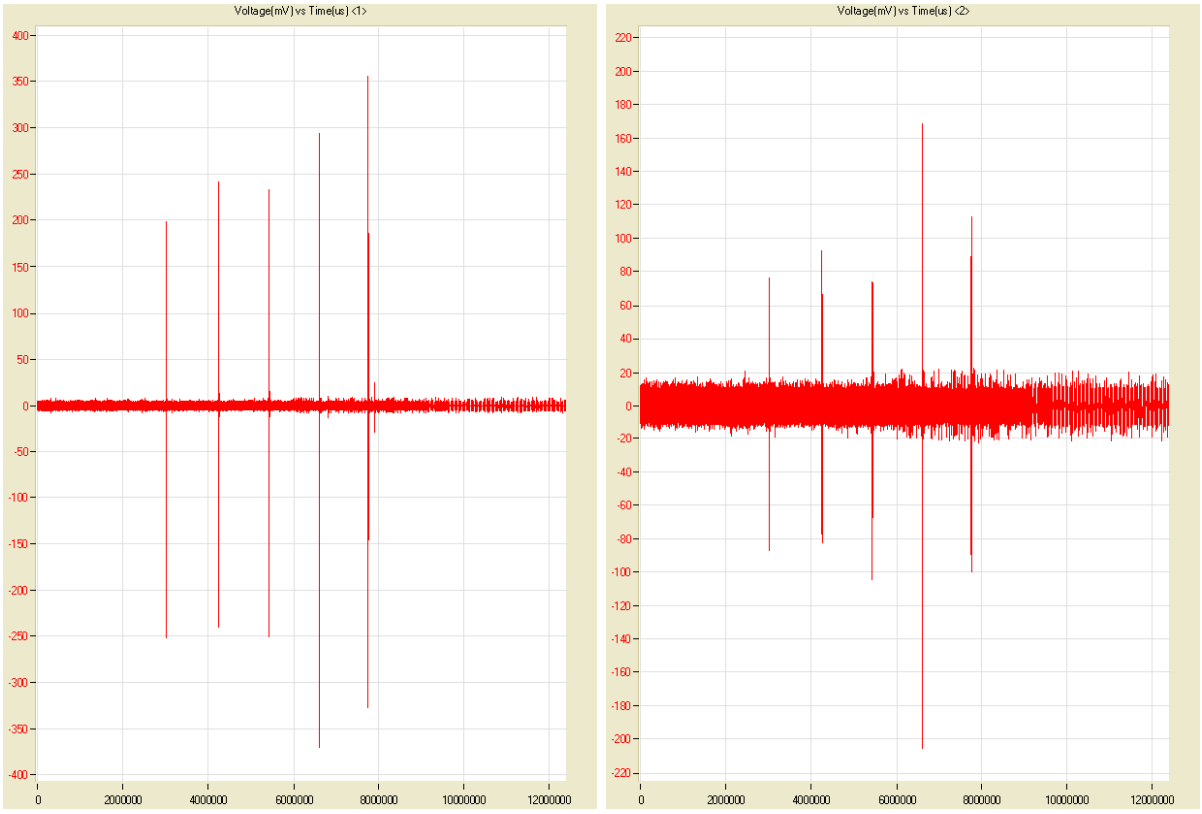

FIGURE 10. AE waves detected by two sensors: left figure is mounted on top, while right bottom

recording result is shown in Figure 12. We can see that two waves are nearly identical in time and amplitude, except for a little difference which may caused by anisotropic conductivity of wood.

4.3. **Damage identification.** In this phase a 10KN load of hardness testing is applied to the specimen, and we set the AE sensor with these parameters (sampling frequency 5M HZ, sampling number 1k, threshold voltage 30dB), and make it transmit all the waves it has captured. Boxwood specimen is subjected to constant pressure until the elastic module of the material is reached and a fracture appears. The experiment results are shown in Figure 13.

Generally speaking, during the experiment process, the acoustic activity (number of AE events that overpass an amplitude threshold) of wood can be classified into three different stages: 1) crack initiation; 2) crack incubation; and 3) crack propagation [23]. Figure 13 shows the evolution of the AE activity during this hardness testing, where the transformation of three crack stages can be easily identified. This result indicates that there are three different AE patterns to be analyzed to characterize each damage stage.

The power spectrums of three stages from this experiment are shown in Figure 14. In stage 1, the amplitudes of AE signals show a maximum around 50kHz [Figure 14(a)]. In stage 2, AE signals have higher amplitudes than in stage 1 and the frequency reaches 500-550kHz [Figure 14(b)]. In stage 3, the amplitudes of AE signals keep almost the same, but the frequency substantially extends to near 1000kHz [Figure 14(c)]. In the light of [24,25], and the results of these experiments, we can conclude that it is entirely possible

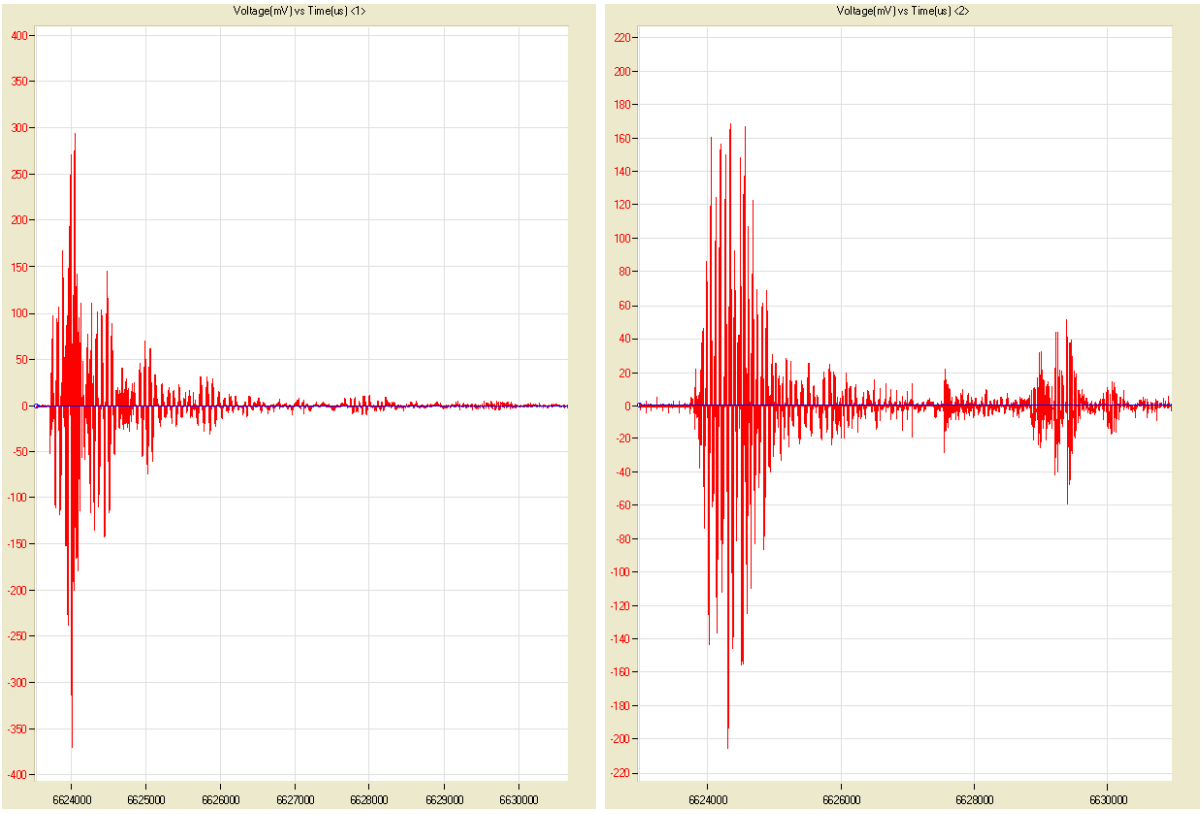

(a) (b)

FIGURE 11. The forth hit waves after magnified

to identify detailed damage status of wooden structure member by using the proposed system.

5. **Conclusions.** The paper presents a prototype wireless two-channel acoustic emission sensor node that supports high sampling rate and high transmission rate, and hence, enables the detection and accurate localization of fracture cracks. The proposed system integrates three different key technologies in a unique sensor device, namely, Wi-Fi communication, difference encoding algorithm, and two-branch dataflow management. It has been demonstrated that this wireless AE sensor system can effectively collect and transmit the AE signal data to control center, also the proposed embedded diagnosis algorithm could make a good use of the spectral content of AE signal, since the different fracture stages analyzed during the experiments show characteristic spectral contents.

Being a first-generation prototype, the current system does have some shortcomings. The energy consumption of the node has not been deeply studied yet. Clearly, for long-term deployment, some form of energy harvesting will be an absolute necessity. The most widely used approach, solar power, has limited applicability here, since the AE sensors are placed in architecture which are completely shaded areas quite frequently. The most promising approach in this domain is to utilize RF energy harvesting. This, however, needs further research. And time synchronization among those wireless nodes in the same network should also be addressed in future.

Acknowledgment. This work is partially supported by the Natural Science Foundation of Jiangsu Province, China (BK20150880). The authors also gratefully acknowledge the helpful comments and suggestions of the reviewers, which have improved the presentation.

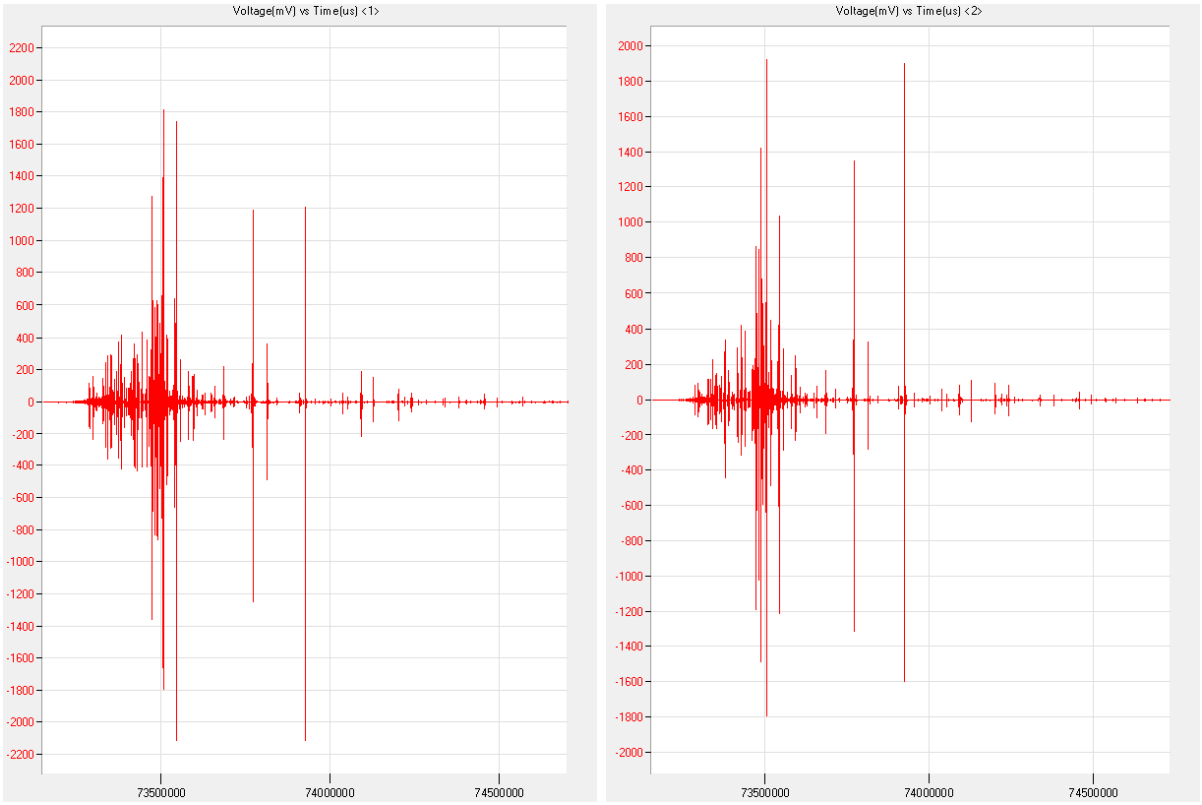

(a) (b)

FIGURE 12. (a) Result of PCI-2 AE system, (b) result of the proposed wireless AE sensor

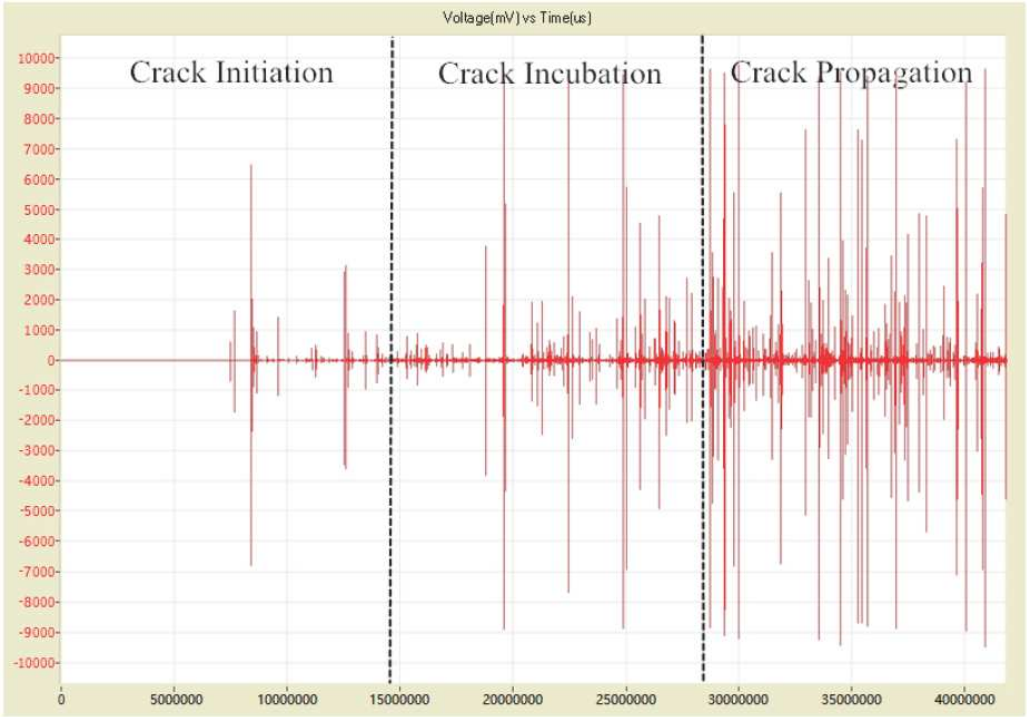

FIGURE 13. AE results in terms of AE voltage versus duration of the hardness test

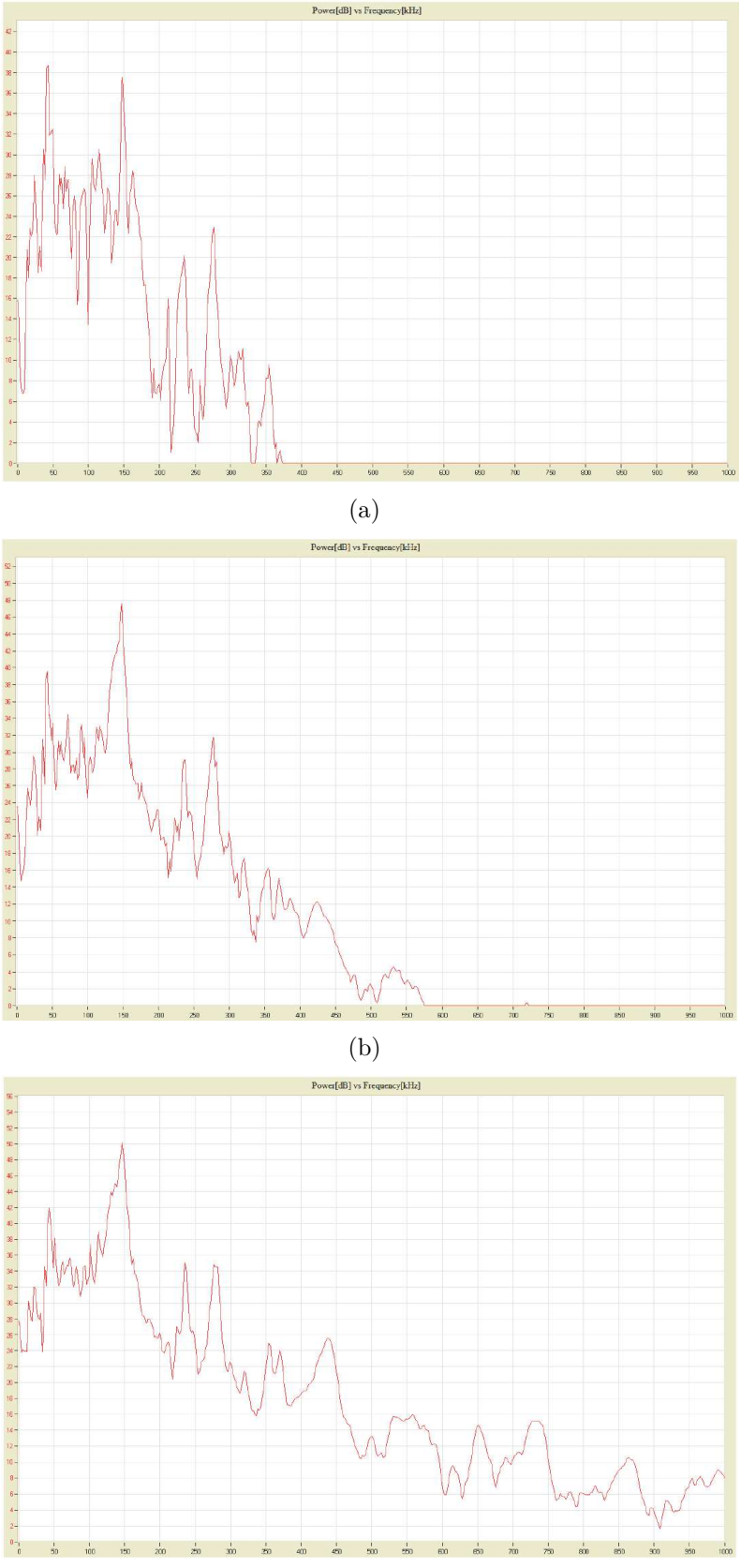

(a)

(b)

(c)

FIGURE 14. Three stages of damage development: (a) crack initiation, (b) crack incubation, (c) crack propagation

REFERENCES

[1] J. Pošta and J. Dolejš, Non destructive assessment of timber elements with an emphasis on radiometry, *International Journal of Architectural Heritage*, vol.9, no.6, pp.655-664, 2015.

[2] L. Girard, J. Beutel, S. Gruber, J. Hunziker, R. Lim and S. Weber, A custom acoustic emission monitoring system for harsh environments: Application to freezing-induced damage in alpine rock walls, *Geoscientific Instrumentation Methods and Data Systems*, no.1, pp.155-167, 2012.

[3] B. V. Hieu, S. Choi, Y. U. Kim, Y. Park and T. Jeong, Wireless transmission of acoustic emission signals for real-time monitoring of leakage in underground pipes, *KSCE Journal of Civil Engineering*, vol.15, no.5, pp.805-812, 2011.

[4] Y. Jin, H. Yang, H. Yang, F. Zhang, Z. Liu, P. Wang and Y. Yang, Nondestructive detection of valves using acoustic emission technique, *Advances in Materials Science and Engineering,* vol.2015, pp.1-9, 2015.

[5] J. Bohse, Acoustic emission, *Handbook of Technical Diagnostics*, pp.137-160, 2013.

[6] B. Aygün and V. C. Gungor, Wireless sensor networks for structure health monitoring: Recent advances and future research directions, *Sensor Review*, vol.31, no.3, pp.261-276, 2011.

[7] C. H. R. Martins, P. R. Aguiar, A. Frech and E. C. Bianchi, Tool condition monitoring of single-point dresser using acoustic emission and neural networks models, *IEEE Trans. Instrumentation and Measurement*, vol.63, no.3, pp.667-679, 2014.

[8] A. Ukil, M. Zlatanski and M. Hochlehnert, Monitoring of HV generator circuit breaker contact ablation based on acoustic emission, *IEEE Trans. Instrumentation and Measurement*, vol.62, no.10, pp.2683-2693, 2013.

[9] J.-H. Zhou, C. K. Pang, Z.-W. Zhong and F. L. Lewis, Tool wear monitoring using acoustic emissions by dominant-feature identification, *IEEE Trans. Instrumentation and Measurement*, vol.60, no.2, pp.547-559, 2011.

[10] A. Ledeczi, T. Hay, P. Volgyesi, D. R. Hay, A. Nadas and S. Jayaraman, Wireless acoustic emission sensor network for structural monitoring, *Sensors Journal IEEE*, vol.9, no.11, pp.1370-1377, 2009.

[11] O. M. Bouzid, G. Y. Tian, J. Neasham and B. Sharif, Envelope and wavelet transform for sound localization at low sampling rates in wireless sensor networks, *Journal of Sensors*, Article ID 680383, pp.1-9, 2012.

[12] O. M. Bouzid, G. Y. Tian, J. Neasham and B. Sharif, Investigation of sampling frequency requirements for acoustic source localization using wireless sensor networks, *Applied Acoustics*, vol.74, no.2, pp.269-274, 2013.

[13] M. D. Prieto, D. Z. Milan, W. Wang, A. M. Ortiz, J. A. O. Redondo and L. R. Martinez, Self-powered wireless sensor applied to gear diagnosis based on acoustic emission, *IEEE Trans. Instrumentation and Measurement*, vol.65, no.1, pp.15-24, 2016.

[14] J. V. Oliver-Villanueva and M. A. Abian-Perez, Advanced wireless sensors for termite detection in wood constructions, *Wood Science and Technology*, vol.47, no.2, pp.269-280, 2013.

[15] Y. Fujii, K. Narahara, Y. Fujiwara, T. Ngatsuma, Y. Yanase, T. Yoshimura, S. Okumura and Y. Imamura, Nondestructive detection of termites using a millimeter-wave imaging technique, *Forest Products Journal*, vol.57, no.10, pp.75-79, 2007.

[16] Y. Yanase, Y. Fujii, S. Okumura and T. Yoshimura, Detection of metabolic gas emitted by termites using semiconductor gas sensors, *Forest Products Journal*, vol.62, no.7/8, pp.579-583, 2012.

[17] Y. Yanase, M. Miura, Y. Fujii, S. Okumura and T. Yoshimura, Evaluation of the concentrations of hydrogen and methane emitted by termite using a semiconductor gas sensor, *Journal of Wood Science*, vol.59, no.3, pp.243-248, 2013.

[18] Y. Wu, Z. P. Shao, F. Wang and G. L. Tian, Acoustic emission characteristics and felicity effect of wood fracture perpendicular to the grain, *Journal of Tropical Forest Science*, vol.26, no.4, pp.522-531, 2014.

[19] B. Kusy, P. Dutta, P. Levis, M. Maroti, A. Ledeczi and D. Culler, Elapsed time on arrival: A simple, versatile, and scalable primitive for canonical time synchronization services, *International Journal of Ad Hoc and Ubiquitous Computing*, pp.239-251, 2006.

[20] C. Yang, X. Zhang, F. Tao and D. C. Lam, A study of the sound transmission mechanisms of a finite thickness opening without or with an acoustic seal, *Applied Acoustics*, vol.122, pp.156-166, 2017.

[21] O. M. Bouzid, G. Y. Tian, K. Cumanan and D. Moore, Structural health monitoring of wind turbine blades: Acoustic source localization using wireless sensor networks, *Journal of Sensors*, vol.2015, Article ID 139695, 2015.

[22] *http://www.physicalacoustics.com/by-product/pci-2/.*

[23] Z. Shi, J. Jarzynski, S. Hurlebaus and L. J. Jacobs, Characterization of acoustic emission signals from fatigue fracture, *Proc. of Inst. Mech. Eng. C, J. Mech. Eng.*, vol.214, no.9, pp.1141-1149, 2000.
[24] Z. Chen, B. Gabbitas and D. Hunt, Monitoring the fracture of wood in torsion using acoustic emission, *Journal of Materials Science*, vol.41, pp.3645-3655, 2006.
[25] A. Reiter, S. E. Stanzl-Tschegg and E. K. Tschegg, Mode I fracture and acoustic emission of softwood and hardwood, *Wood Science and Technology*, vol.34, pp.417-430, 2000.